

Magnetic Bubble Materials

Edward A. Giess

Bubble domains are small, magnetized, mobile regions within sheets or films of certain magnetic materials. The presence of a bubble can represent a binary "bit" of information, a one, and its absence a zero. Memory and recording devices marketed today store and move a million bubbles, each ≈ 2 micrometers in diameter, within a film ≈ 2 micrometers in thickness and less than 1 square centimeter in area. These solid-state de-

the south poles on the other surface. In this case the sheet is magnetically uniaxial. There is only one significant axis, the one normal to the sheet. The magnetization lies within the sheet in a direction perpendicular to the plane of the sheet (see arrows in Fig. 1). Sectional magnetic walls could form within the sheet, separating it into magnetic domains where adjacent domains have antiparallel magnetizations. Walls are finite

Summary. Physicists, materials scientists, and engineers combined to bring solid-state bubble devices into the computer memory and recording marketplace. Devices with smaller bubbles are being developed for increased data capacity and lower cost. Epitaxial garnet films made by isothermal dipping in molten solutions helped put the technology in place and will probably satisfy the material needs of future devices with bubbles scaled down from 2 to 0.5 micrometer in size.

vices can be made smaller in size and in data capacity; thus smaller, more economical units can be assembled than for the motor-driven disks and tapes they may replace. Devices promise to be especially useful in computer terminals and small data processors. To increase the data capacity of devices and to decrease their cost, the technology is moving toward devices with smaller bubbles in thinner films.

In this article, magnetic bubbles, the devices using them, and the physics of bubbles will be discussed first. Next, the physical forms of bubble materials—platelets and films—that have influenced the evolution of devices will be considered. Finally, materials will be described, especially the magnetic garnet films, which have been the main bubble material and probably will continue to be for quite a while.

Magnetic Bubbles

If a bar magnet were flattened and thereby drastically shortened along its north-south polar axis, into a thin sheet, it would have a large (shape anisotropy) magnetostatic energy from the numerous north poles on one surface opposed by

in thickness and have a magnetic energy of their own, but they reduce the net energy and thereby increase the stability of the total magnetic configuration. Neighboring domains have opposite north-south poles at the sheet surfaces and neighboring flux lines can easily close upon each other. Domains are stripe-shaped, and half of them are magnetized north, while the other, intervening half are magnetized south (Fig. 1a).

Stripe domains can be observed directly with a microscope in thin transparent magnetic sheets (such as the garnet films presently used in devices) because the Faraday effect rotates the plane of transmitted polarized light depending on the direction of magnetization in individual domains. This visibility of individual domains has contributed greatly to the rate of development of bubble technology.

A perpendicular bias field—for example, from parallel external permanent magnet sheets—will favor and thereby increase the area of domains magnetized in the same direction, while it will decrease the area of adjacent domains magnetized oppositely. At a certain bias (strip-out) field, the unfavored stripe domains will shrink into right-cylindrical domains called bubbles (*1*). An impor-

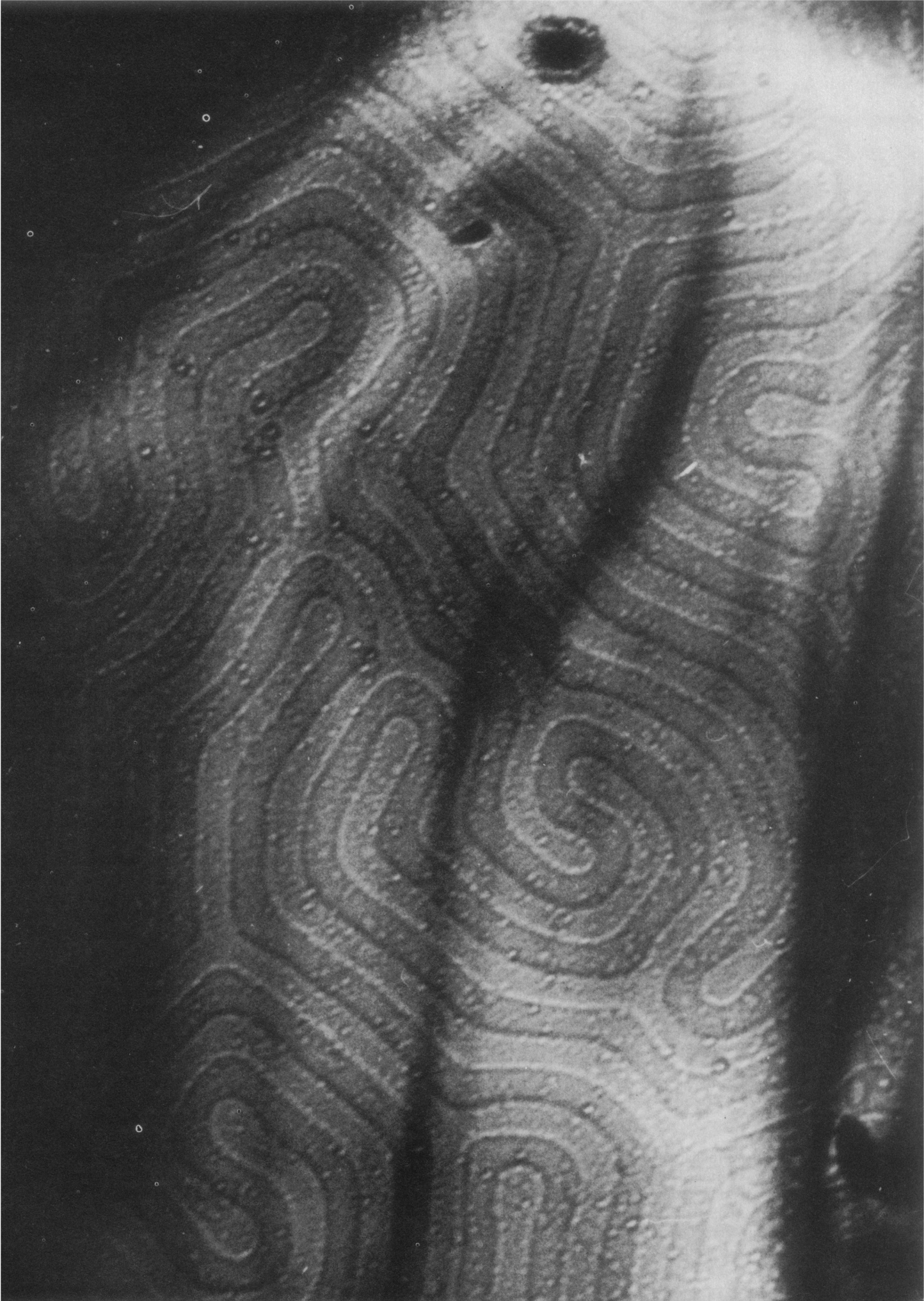
tant property of these bubbles is their ability to be moved laterally through the sheet. In commercial devices this propagation is induced by a thin-film array of metal magnets deposited atop the bubble film. The array is controlled by an in-plane magnetic field applied with two external coils.

Bubble Devices

Devices (2, 3) must be provided with means for the generation, moving, switching (transfer), sensing, and annihilation of bubbles. Typically, all these device operational functions are achieved with tiny Permalloy (Ni,Fe) soft magnets (which can easily change their direction of magnetization) and electrical conductor lines about $0.2 \mu\text{m}$ thick deposited on a $0.15\text{-}\mu\text{m}$ SiO_2 layer atop the bubble storage layer (Fig. 2). These metallurgical patterns are shaped by optical lithography techniques (*4*), whose resolution currently limits C-bar (asymmetric chevron) Permalloy magnets to a minimum lateral gap spacing of about $1 \mu\text{m}$ between adjacent C-bars. The bubble diameter must be about twice this minimum gap. In a propagation and storage track, C-bars that can host one bubble each are aligned along a common axis with a repeat distance of four to five times a bubble diameter. Bubbles rest beneath the C-bars in the gap region, and they propagate when the in-plane drive field rotates and changes the magnetic polarity of the Permalloy C-bars, thereby alternately attracting and repelling the bubbles. Since the stabilizing bias field is supplied by permanent magnets, bubbles are nonvolatile (that is, they continue to exist even after external electrical power is disconnected), and they can be migrated through the device in the solid state without any mechanically moving parts such as are required to move information in conventional disk and tape technologies.

One bubble can be formed and those in the device advance one position with each rotation of the drive field, which determines the device frequency of operation (about 100 kilohertz). An electrically pulsed conductor line chops bubbles from a seed bubble in the generator, and then they are fed into a major track of C-bars (see Fig. 3). A series of orthogonal minor loop tracks face the major track along its length and are connected to it through a series of switching Permalloy patterns actuated by a transfer con-

The author is a research staff member at the IBM T. J. Watson Research Center, Yorktown Heights, New York 10598.



ductor line, so that bubbles can be transferred back and forth between the major track and the minor storage loop. Having minor loops reduces the time needed to access data. At the end of the major track, bubbles are read by a sensor conductor line attached to the ends of a thin-layer Permalloy strip whose resistance decreases in the magnetic field of a bubble. Finally, the bubbles can be eliminated by an annihilator pattern.

Bubble Physics

A magnetic bubble is a physical phenomenon not unique to any one class of chemical compositions. [However, at present practically all bubble devices are made with single-crystal films of multicomponent magnetic rare earth-iron oxides having the garnet structure (5).] Bubble physics (6) considerations dominate device design and materials selection. The stability, size, and speed of bubbles are the key design parameters affecting device reliability, capacity, and data rate, respectively. Stability refers to how well bubbles resist destruction by environmental perturbations, such as the drive fields used to propagate domains. Smaller bubbles are packed more densely and thereby increase data capacity. Since small bubbles are more closely spaced, they move shorter distances and give better data rates than large bubbles with the same velocity. Also, of course, increased bubble velocity improves the data rate in a device. (In present-day devices, the coil drive circuitry limits the data rate.)

Stability of bubble domains is measurable by the in-plane field H_u (called the anisotropy field) required to tip the magnetization M from its easy axis by 90° into the film plane. The product $H_u M/2$ is the uniaxial anisotropy energy constant K_u . (In some bubble materials, this magnetic anisotropy can have three components: growth-induced, strain-induced, and intrinsic.) The stability factor is defined as the ratio of H_u to saturation magnetization, or in energy terms as

$$Q \equiv \frac{K_u}{2\pi M_s^2} \quad (1)$$

the ratio of the anisotropy energy to the magnetostatic energy. For stable isolated bubbles to exist, Q must be greater than unity. Furthermore, unless Q is appreciable, the in-plane drive field can strip out bubbles into stripes, a failure mode for devices. Stable bubbles exist in a range of bias fields between the (higher) collapse field H_0 , where the entire film becomes a single domain, and the

(lower) strip-out field (about $0.7 H_0$), where bubbles change back into stripe domains. Depending on film material parameters and thickness, H_0 is 0.4 to 0.6 of $4\pi M_s$, the saturation magnetization.

The film thickness is generally made to be just less than the bubble diameter for energetic and stability reasons, and the bubble diameter is about eight times the characteristic length

$$\ell = \frac{\sqrt{AK_u}}{\pi M_s^2} \quad (2)$$

where A is the magnetic exchange stiffness constant, which is a measure of how strongly neighboring ions are magnetically coupled. The characteristic length is the ratio of the domain wall energy to the demagnetization energy, which is directly related to the magnetostatic energy. Equation 2 shows that bubble size is determined mainly by magnetization. The important thing to remember is that smaller bubbles require larger magnetization.

From a materials standpoint, the data rate of a device and the time required to

access data are governed by the speed of bubbles. It will be seen that stability and speed have contrary materials requirements. Stability demands relatively high anisotropy, and speed needs low anisotropy. The speed of a bubble is determined by the product of the drive field across the bubble minus the threshold field for movement (coercivity) and the bubble mobility (velocity per drive field gradient)

$$\mu = \frac{\gamma}{\alpha} \sqrt{\frac{A}{K_u}} \quad (3)$$

where γ is the gyromagnetic ratio, which has to do with the dynamics of atoms changing their directions of magnetization, and α is the Gilbert damping (magnetic viscosity) parameter. The quantity $\sqrt{A/K_u}$ times π is the domain wall width within which the magnetization reverses direction in any one or a combination of possible wall magnetic structures. For example, simple bubbles have a Bloch wall, wherein the magnetization vector rotates in the plane of the wall in either a left- or right-handed (chirality) direction, but in a Néel wall, which can partly form near the film surfaces, the magnetization vector rotates directly into the wall. Different structures within a given wall meet along Bloch lines, which can meet at Bloch points. These magnetic wall structures provide a mechanism for information coding of a higher order than binary (7).

Walls, whether simple or complex, define bubbles, and defects that lie in the plane of a wall are particularly effective in blocking bubble motion. Accordingly, films for devices must have a high degree of physical perfection and freedom from flaws. The growth techniques developed for making garnet films and the properties of garnets themselves provide products with the high quality required for devices.

Platelets and Films

The early devices had large bubbles and were made with platelets cut and polished from large single crystals. Now competition from other technologies creates the need for devices with smaller bubbles in thinner sheets, which are produced as thin films on flat substrates. Today, magnetic garnet films are grown as single-crystal layers, which are a crystallographic continuation of single-crystal substrates that are nonmagnetic platelets. This process for making films is called epitaxy.

Bubbles have been studied in single-crystal platelets of Fe_2O_3 -based compounds with magnetoplumbite, orthofer-

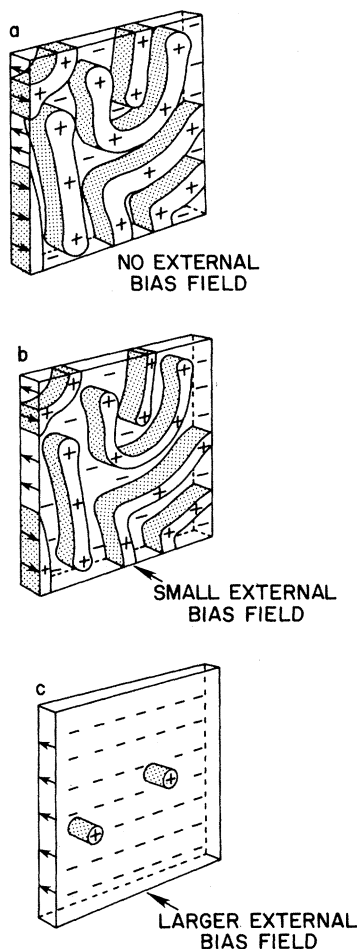


Fig. 1. Magnetic domains in a uniaxial sheet under the influence of an external bias field. [Reprinted from Bobeck and Scovil (22). Copyright © Scientific American, Inc., 1971. All rights reserved.]

rite, and garnet crystal structures and in single-crystal films of the latter. Also, films based on metallic $GdCo_5$ alloy compositions (8) with a glasslike amorphous structure have been used. Devices have been fabricated with all but the magnetoplumbites.

Amorphous films were developed late and have bubble properties that are susceptible to temperature change in larger bubble films; hence they could not displace garnet films, which have satisfied design needs to date. Amorphous films could be revived for future devices using very small bubbles, but they would require an electrical insulation layer because they are conductors.

It is possible to slice and polish bulk crystal platelets, 1 cm^2 in area, down to a thickness of about $25\ \mu\text{m}$; this sets a similar minimum bubble diameter, which in turn limits data storage density. A pref-

erable technology, which considerably relieves both the areal and thickness constraints, is to grow magnetic films epitaxially on thicker nonmagnetic crystal substrate wafers that have the same crystallographic structure and lattice spacing. An epitaxial film has chemically different, but similarly sized, ions in exact positional registration with ions in its supporting substrate lattice. Fortunately, the nonmagnetic gallates (Ga_2O_3 -based compounds) have a crystal chemistry related to that of ferrites, and they function well as substrates in the case of garnets. Both Ga and Fe prefer to be trivalent and have similar ionic radii.

Magnetoplumbite, orthoferrite, and garnet crystals (9) can all be obtained from the pseudoternary $RE_2O_3\text{-}Fe_2O_3\text{-}PbO$ system, where RE is a rare earth or Y (see Fig. 4). In this system the fluxing action of PbO lowers crystallization tem-

peratures below the range where Fe^{3+} tends to be chemically reduced Fe^{2+} unless the oxygen pressure is considerably greater than atmospheric. The latter effect causes magnetoplumbite and iron garnets to melt incongruently—that is, to melt into a liquid, but also into a new solid phase as well, each having a different composition. Consequently, garnet ($RE_3Fe_5O_{12}$) crystals are grown from molten solutions with $Fe_2O_3 : RE_2O_3$ ratios much greater than the 5:3 stoichiometric ratio.

Bulk crystals and epitaxial films of Fe_2O_3 -based compounds grow from PbO-fluxed melts (molten solutions) at linear growth rates around $1\text{ cm per }10^6$ seconds; thus it takes at least 1 week to grow a bulk crystal but only several minutes to produce a thin film. The same physical process that is too slow to produce economical bulk crystals allows enough time to make films in a controlled and reproducible way. Crystals of $Gd_3Ga_5O_{12}$ garnet (GGG) (substrates for magnetic garnet epitaxial films), on the other hand, are pulled at almost 1 cm per hour from GGG melts as right cylinder-shaped boules by the Czochralski technique. Substrates of device films are hundreds of times thicker than their films. Fortunately for the sake of economy, substrate boules can be grown hundreds of times faster than films because boules grow from GGG melts with the same composition. Unlike iron garnets, GGG melts congruently. The same Czochralski apparatus geometry is employed with different materials to grow semiconductor silicon boules. Furthermore, the development of garnet epitaxial film technology was accelerated by processing GGG substrate wafers with essentially the same diamond saws and chemical-mechanical polishing equipment that existed for processing Si wafers. Also, the development of yttrium aluminum oxide garnet (YAG) boules for lasers helped pioneer the growth techniques for GGG boules, which are now grown as large as 7.5 cm in diameter routinely.

Materials

Magnetoplumbite is hexagonal (uniaxial) and is one of a class of so-called hexaferrites, wherein Pb can be replaced by Sr or Ba. Isolated bubbles were first observed (9) in 1960 in single-crystal platelets of magnetoplumbite ($PbO \cdot 6Fe_2O_3$), although their device potential was not recognized until later. Ten years later it was shown that bubbles in other hexaferrites have limiting ve-

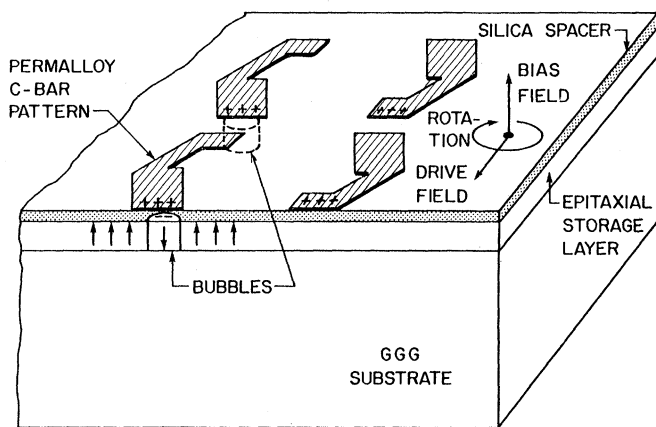


Fig. 2. Conventional field-accessed bubble device chip (schematic section). [Reprinted from George and Reyling (3). Copyright © Mc-Graw-Hill, Inc., 1979. All rights reserved]

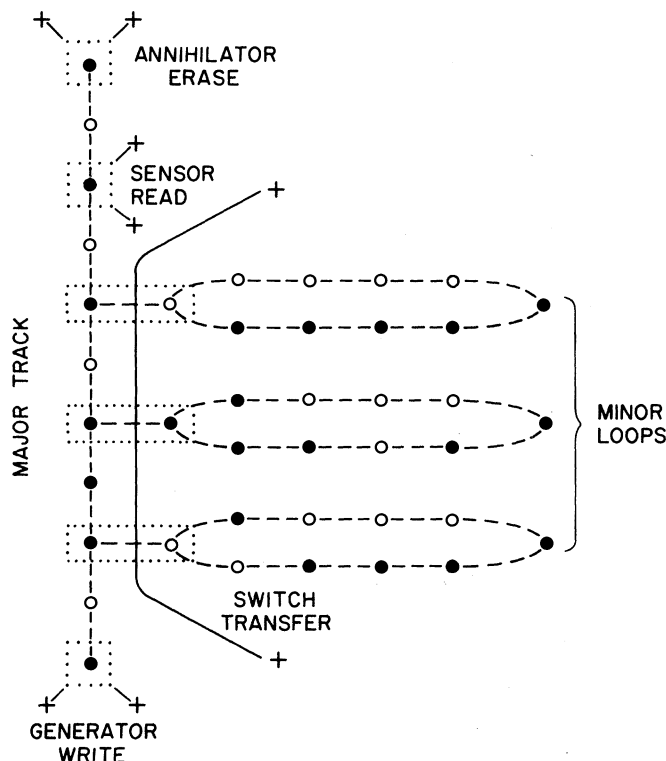


Fig. 3. Conventional device chip organization (schematic).

locities too low (< 600 cm/sec) for bubble devices (10). However, it has never been demonstrated that this limitation is intrinsic to hexaferrites, some of which do function in high-frequency microwave devices. It may be possible to make useful submicrometer bubble devices, given the correct hexaferrite chemical composition in the form of a physically perfect epitaxial hexaferrite film. It is not obvious what crystal would be a suitable substrate.

Orthoferrites, with the general formula $REFeO_3$, were the first materials employed in bubble devices (1). Platelets $100 \mu\text{m}$ thick and containing bubbles $100 \mu\text{m}$ in diameter were used. They served well as bubble materials for early engineering studies, but were soon replaced by garnets because orthoferrites have a limited range of low $4\pi M$ values, resulting in large bubbles.

Garnets have a cubic crystal structure and consequently are not intrinsically uniaxial. They became the dominant bubble materials after it was found that certain magnetic garnets can have growth-induced uniaxial anisotropy K_g when grown from molten solutions (11). Both bulk and epitaxial crystal films exhibit this phenomenon in the absence of macroscopic stress. Despite the importance of anisotropy to the existence of stable bubbles, two other considerations are given at least as much attention in designing garnet compositions for bubble devices. The first is magnetization, which is the principal factor in determining bubble size and is adjusted mainly by partially substituting nonmagnetic Ga or Ge for magnetic Fe. The second is the film lattice parameter, which must closely match that of the substrate and is adjusted mainly by a critical admixture of two or more rare earths.

Magnetic Garnet Crystal Chemistry

Compared to the garnets found in nature, magnetic garnets have the same arrangement of atoms, but different kinds of atoms. Magnetic garnet films and their substrate crystals contain yttrium or rare earths and iron or gallium oxides while natural garnets usually contain calcium, aluminum, and silicon oxides.

The garnet structure belongs to the highest symmetry and most complex space group $Ia\bar{3}d$. The unit formula for yttrium iron garnet (YIG) is $\{Y^{3+}\}_3\text{[Fe}^{3+}\text{]}_2(\text{Fe}^{3+})_3\text{O}_{12}^{-2}$. There are three types of cation sites designated as follows: {dodecahedral} with eight oxygen ion nearest neighbors, [octahedral] with six, and {tetrahedral} with four.

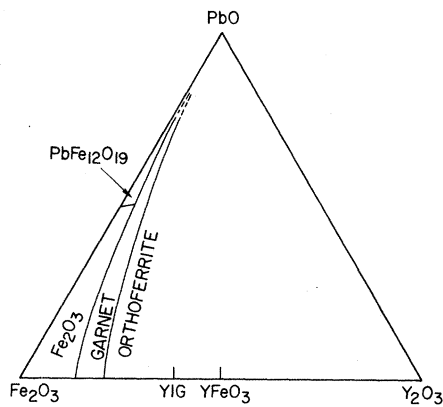


Fig. 4. Pseudoternary $PbO\text{-}Y_2O_3\text{-}Fe_2O_3$ phase equilibrium diagram showing magnetoplumbite, $PbFe_{12}O_{19}$; hematite, Fe_2O_3 ; garnet, $Y_3Fe_5O_{12}$ (YIG); and orthoferrite, $YFeO_3$ primary phase areas. Any possible combination of the three constituents at the apexes of this composition triangle can be represented by a point within the triangle. The areas of this phase diagram are labeled according to the first (primary) crystal phase that will freeze on cooling a molten solution whose composition point is in the area. [Reprinted from Nielsen and Dearborn (23). Copyright © Pergamon Press, Inc. 1958]

Each garnet unit cell contains eight formula units—for example, $Y_{24}Fe_{40}O_{96}$, which has a 1.2376-nanometer repeat distance. The high symmetry and large lattice spacing probably account for the crystals' reluctance to nucleate from solution spontaneously or form imperfections such as dislocations. Both tendencies aid the controlled growth of substrate crystals and magnetic bubble films with the high physical perfection required for devices.

A very considerable number and range of possible chemical substitutions (12) provides the basis for selecting homogeneous solid solutions useful in bubble devices—for example, {Y, La to Lu, Bi, Ca, Pb}, [Fe, Mn, Sc, Ga, Al], and (Fe, B, Ga, Al, Ge). Each Fe^{3+} ion in the crystal acts as a single magnet with a net magnetic moment. Within each domain, all $[Fe^{3+}]$ have parallel magnetic moments, as do all (Fe^{3+}) , but the octahedral and tetrahedral moments have antiparallel alignment, so there is a net magnetization M , the difference between the two sublattices. These magnetic sublattices are coupled by the exchange energy, which decreases with increasing temperature. At the Curie temperature, thermal energy finally breaks the magnetic coupling and M goes to zero. Bubble diameter (Eq. 2) is smallest, about $0.5 \mu\text{m}$, for the simple undiluted $RE_3Fe_5O_{12}$ garnets, where RE is Y or a rare earth, because $4\pi M$ is a maximum, about 1800 gauss (= 0.18 tesla). The magnetic {RE = Sm to Yb} ions, when substituted, have their own magnetic sublattice,

which couples antiparallel to the (Fe) and thereby reduces $4\pi M$. However, bubble diameter is principally adjusted (increased) in garnets by nonmagnetic (Ga^{3+}) or (Ge^{4+}) partial substitutions for (Fe^{3+}), which reduce $4\pi M$. When tetravalent (Ge^{4+}) is substituted, its charge must be compensated by an equal amount of $\{Ca^{2+}\}$ in the otherwise trivalent cation garnet lattice.

The substantial Ca-Ge and especially Ga substitutions necessary to obtain a low $4\pi M$ (< 200 gauss) for early $\sim 6\text{-}\mu\text{m}$ bubble devices also reduced the Curie temperature sufficiently to make the devices sensitive to ambient temperature fluctuations. This problem is less evident in today's $\sim 2\text{-}\mu\text{m}$ bubble devices and will be less so in future devices with smaller bubble garnet compositions. It is not practical to obtain smaller bubbles by increasing $4\pi M$ with nonmagnetic (Sc^{3+}) substitutions for octahedral Fe^{3+} because the Curie temperature is concurrently sharply reduced.

The rare earths Sm and Eu are the most effective promoters of K_g , the growth-induced K_u , when the growth direction is [111] or [100]. Either of these large RE ions combined in a 50:50 ratio with a smaller one (Tm, Yb, or Lu) produces the maximum K_g in (111) films (13), but reducing their concentration diminishes K_g approximately linearly in (100) films (14). Both Sm and Eu dampen domain wall motion (decrease data rate), which means that compositions with more nonmagnetic ions (such as Lu or Y) are to be favored. Also, Sm and Eu enhance the intrinsic magnetocrystalline anisotropy K_1 , which favors [111] as the easy direction of magnetization. Mainly because of growth and crystalline anisotropy, nearly all early garnet devices were oriented (111). Crystalline anisotropy contributes proportionately less to the total anisotropy for smaller bubble garnets. Mechanical in-plane strain arising from a lattice spacing mismatch between an epitaxial film and its substrate must be less than $\sim 10^{-3}$ (lattice matching is achieved without difficulty because films are multicomponent). Mismatch strain can be tensile or compressive and can produce a stress-induced anisotropy K_s ; this is positive or negative depending on the film magnetostrictive coefficient, which is the summation of contributions from constituent magnetic ions. Bubble stability is principally realized through K_g with K_1 and K_s making at best minor contributions. This is especially true for small-bubble films, which require very high K_u for stability, and consequently the number of useful small-bubble garnet compositions is limited.

Epitaxial Garnet Films

The success of magnetic bubble technology is in no small measure a result of the physical quality, lateral uniformity, and wafer-to-wafer reproducibility of epitaxial garnet films. These films are grown by dipping axially rotated substrate wafers (Fig. 5) into isothermal molten solutions of garnet. A horizontal rotating wafer behaves like a centrifugal fan that draws solution upward in a central plume beneath the wafer and expels the solution radially across the underside of the wafer. This fluid flow leads to a steady-state regime that produces films of the desired quality, mainly because the film growth rate is constant. The film growth process is fairly well understood now and is interesting in its own right (15) because it is possible to both control and measure precisely film growth-related parameters. This and other liquid phase epitaxy processes (such as those used to make GaAs films) are often called LPE processes.

It is appropriate to consider briefly some substrate factors that contribute to the success of garnet LPE. Given the magnetic orientation requirements for garnets, it is fortunately most economical to pull (grow) GGG boules along [111] or [100] axes, the fast growth directions, and then to cut them with a diamond saw normal to their (growth) axes into disk-shaped wafers 0.05 cm thick. This takes advantage of the natural circular shape of boule sections, a shape useful in film growth. It also minimizes the effect of planar striations, which lie in the plane of each disk and arise from slight Gd:Ga stoichiometry fluctuations in the boule growth interface. The fluctuations exist because GGG is a solid solution and the most stable (maximum melting) composition is slightly enriched in Gd_2O_3 .

Although much of the crystal chemistry of magnetic garnets was developed for earlier microwave devices with bulk crystals grown from molten salt solutions, the technologically important supercooling tendency of these PbO-fluxed melts was recognized (16) only after epitaxial film growth was attempted for bubbles. Without causing crystals to nucleate spontaneously, the molten solutions can be supercooled as much as 100°C below their saturation temperatures T_s , where garnet crystals would begin to nucleate and to grow if equilibrium conditions were easy to attain. Solutions will remain in this metastable crystal-free state for hours if undisturbed. However, in garnet LPE, the metastable solutions are disturbed and growth is triggered on a GGG wafer (a nucleus) when it is

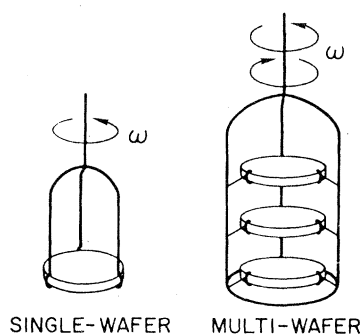


Fig. 5. Substrate assemblies for horizontal plane dipping with rotation ω of single and multiple wafers. These assemblies are lowered into supersaturated garnet solutions in open platinum crucibles.

dipped into the solution. In 30 to 300 seconds epitaxial films will generally achieve sufficient thickness for device applications. Isothermal growth temperatures T_g nearer to T_s —for example, with undercoolings $\Delta T = (T_s - T_g)$ of about 15° to 50°C (15)—are generally used. Isothermal growth in molten solutions supersaturated by supercooling is simpler than growth in conventional systems supersaturated by dynamic cooling, which requires massive heat flow and temperature gradients that depend on apparatus geometry and sophisticated controls.

Growth depletes solute (nutrient) from the solution adjacent to the growth interface, thereby creating a diffusion boundary layer across which solute species subsequently must diffuse to the interface from the bulk of the solution. Control of the boundary layer thickness is the key to a constant growth rate and compositional homogeneity of films. Growth is impeded not only by the growth interface reaction incorporating garnet into the solid but also by transport across the diffusion boundary layer, whose thickness δ can be regulated and made uniform by forced solution flow. The appropriate solution flow pattern is obtained when disk-shaped GGG wafers are rotated singly or oscillated angularly in a multiple coaxial array (Fig. 5) with an angular velocity ω . Without solution flow δ^2 is proportional to growth time t , and the growth rate decreases with time, resulting in nonuniform film compositions.

With forced flow induced by rotation δ^2 is inversely proportional to ω , which is made constant, and growth rate f^+ attains a steady-state value.

$$f^+ \cong (C_L - C_e) \frac{D}{\delta} \frac{1}{1+r} \quad (4)$$

where C_L is the garnet concentration in the bulk liquid, C_e is the equilibrium concentration (17), and r is the ratio of D/δ to

K , the interface reaction constant. The critical diffusion constant D is that of the slowest moving species. The diffusion boundary layer is not equivalent to the hydrodynamic one, but they are coupled. (When r is large the interface reaction dominates growth.)

For isothermal growth, this gives a constant f^+ , which ensures homogeneous film composition for the multiconstituent (solid solution) garnet systems used in devices. The ratio of constituents in solid solution crystals will change with f^+ and T_g by the so-called segregation effect, which is pronounced in slow-growth processes such as this (18). As growth rate is increased, the crystal composition tends toward that of the solution. Therefore, faster growth leads to more Pb from the solution being incorporated into the crystal.

Both diffusion and reaction are thermally activated, the reaction being especially sensitive to temperature. The diffusive transport process tends to limit growth and therefore predominates at higher growth temperatures ($\approx 900^\circ\text{C}$), whereas the interface reaction is rate-determining at lower T_g values. When diffusion is significant, even with forced solution flow, there is a transient epitaxial layer up to about 0.2 μm thick formed during the growth start-up when the boundary layer itself is forming. In this very short time period, the interface reaction essentially alone impedes growth. Therefore the transient layer adjacent to the substrate grows with a very high f^+ , giving rise to a different composition than that of the bulk film. The transient layer typically contains more Pb^{2+} (solvent) in solid solution and might adversely affect future small bubble films, which will have to be thinner ($< 1 \mu\text{m}$ thick). Growth conditions favoring reaction over transport—that is, where r in Eq. 4 is large—will suppress the transient. These conditions will be required for the very small bubble films of the future.

Future

Smaller bubbles in thinner garnet films are going to be required. Future epitaxial films made by extending the PbO molten solution technology will probably be grown from more dilute solutions at lower growth temperatures and lower rates, but at larger undercoolings. These garnets will have higher $4\pi M$ and anisotropy, but will be similar to present garnets. Higher magnetization will come from less dilution of the iron lattices with nonmagnetic ions, and probably slightly

more Sm (or Eu) will be used for the anisotropy. Conventional Permalloy devices with 2- μm bubbles are approaching bit density limitations imposed by optical lithography and are therefore unlikely to test the limit of available 0.5- μm bubble garnet materials (19). On the other hand, contiguous disk devices (20) have propagation patterns that somewhat relieve lithographic constraints and are taking bubbles into the submicrometer range with conventional field-access technology at hundred-kilohertz data rates. A newly proposed current-access approach (21) has the potential of achieving megahertz data rates. These device engineering considerations can be expected to receive more immediate attention (with only modified garnets) than any search for new materials.

References and Notes

1. A. H. Bobeck, *Bell Syst. Tech. J.* **46**, 1901 (1967).
2. J. A. Rajchman, *Science* **195**, 1223 (1977); R. Kowalchuk, W. S. Chen, T. Mendel, J. Neuhau- sel, *Circuits Manuf.* **19**, 22 (September 1979); G. Cox, *Electron. Des.* **24**, 154 (22 November 1979).
3. P. K. George and G. Reyling, Jr., *Electronics* **52**, 99 (2 August 1979).
4. T. C. Penn, *Science* **208**, 923 (1980).
5. The following are detailed reviews on magnetic bubble materials: J. E. Davies and E. A. Giess, *J. Mater. Sci.* **10**, 2156 (1975); J. W. Nielsen, *IEEE Trans. Magn.* **MAG-12**, 327 (1976); V. N. Dudorov, V. V. Randoshkin, R. V. Telesnin, *Sov. Phys. Usp.* **20**, 505 (1977); S. L. Blank, in *Crystal Growth: A Tutorial Approach*, W. Bardsley, D. T. J. Hurle, J. B. Mullin, Eds. (North-Holland, Amsterdam, 1979), p. 241; A. H. Eschenfelder, *Magnetic Bubble Technology* (Springer-Verlag, New York, 1980); J. W. Nielsen, in *Annual Review of Materials Science*, R. A. Huggins, R. H. Bube, D. A. Vermilyea, Eds. (Annual Reviews, Palo Alto, Calif., 1979), vol. 9, p. 87; P. Chaudhari *et al.* (8).
6. A. A. Thiele, *Bell Syst. Tech. J.* **48**, 3287 (1969); *J. Appl. Phys.* **41**, 1139 (1970).
7. T. J. Beaulieu, B. R. Brown, B. A. Calhoun, T. L. Hsu, A. P. Malozemoff, *AIP Conf. Proc. No. 34* (1976), p. 138.
8. P. Chaudhari, J. J. Cuomo, R. J. Gambino, E. A. Giess, in *Physics of Thin Films*, G. Hass, M. H. Francombe, R. W. Hoffman, Eds. (Academic Press, New York, 1977), vol. 9, p. 263.
9. C. Kooy and U. Enz, *Philips Res. Rep.* **15**, 7 (1960).
10. A. H. Bobeck, *IEEE Trans. Magn.* **MAG-6**, 445 (1970).
11. ———, E. G. Spencer, L. G. van Uitert, S. C. Abrahams, R. L. Barns, W. H. Grodkiewicz, R. C. Sherwood, P. H. Schmidt, D. M. Smith, E. M. Walters, *Appl. Phys. Lett.* **17**, 131 (1970).
12. S. Geller, *Z. Kristallogr.* **125**, 1 (1967); W. Tolksdorf, in *Landolt-Börnstein: Numerical Data and Functional Relationships in Science and Technology* (Springer-Verlag, New York, 1978), new series, group 3, vol. 12, part a.
13. E. J. Heilner and W. H. Grodkiewicz, *J. Appl. Phys.* **44**, 4218 (1973).
14. T. S. Plaskett, E. Klokholm, D. C. Cronemeyer, P. C. Yin, S. Blum, *Appl. Phys. Lett.* **25**, 357 (1974).
15. E. A. Giess and R. Ghez, in *Epitaxial Growth*, J. W. Matthews, Ed. (Academic Press, New York, 1975), p. 183; W. van Erk, *J. Cryst. Growth* **43**, 446 (1978).
16. H. J. Levinstein, S. Licht, R. W. Landorf, S. L. Blank, *Appl. Phys. Lett.* **19**, 486 (1971); J. E. Davies and E. A. Giess, *J. Cryst. Growth* **30**, 295 (1975).
17. The term $C_L - C_e$ can be given as

$$C_L \left(\frac{1}{T_g} - \frac{1}{T_s} \right) = C_L \frac{\Delta T}{T_g T_s}$$
 The equilibrium concentration is determined by T_g .
18. W. van Erk, *J. Cryst. Growth* **46**, 539 (1979).
19. E. A. Giess, R. J. Kobliska, F. Cardone, *J. Appl. Phys.* **50**, 7818 (1979); T. S. Plaskett *et al.*, *ibid.*, p. 7821; E. A. Giess and R. J. Kobliska, *IEEE Trans. Magn.* **MAG-14**, 410 (1978).
20. Y. S. Lin, G. S. Almasi, G. E. Keefe, E. W. Pugh, *IEEE Trans. Magn.* **MAG-15**, 1642 (1979).
21. A. H. Bobeck, S. L. Blank, A. D. Butherus, F. J. Ciak, W. Strauss, *Bell Syst. Tech. J.* **58** (part 2), 1453 (1979).
22. A. H. Bobeck and H. E. D. Scovil, *Sci. Am.* **224**, 78 (June 1971).
23. J. W. Nielsen and E. F. Dearborn, *J. Phys. Chem. Solids* **5**, 202 (1958).
24. The author has been fortunate to have many competent co-workers and to have interacted with others externally over the last decade of bubbles studies. It is a pleasure to acknowledge helpful comments and suggestions from G. S. Almasi, H. Chang, A. H. Eschenfelder, R. Ghez, C. F. Guerci, G. Keefe, R. J. Kobliska, Y. S. Lin, A. P. Malozemoff, E. McCarthy, T. S. Plaskett, E. W. Pugh, L. L. Rosier, M. W. Shafer, and M. B. Small.